Liu et al., https://doi.org/10.1083/jcb.201705116

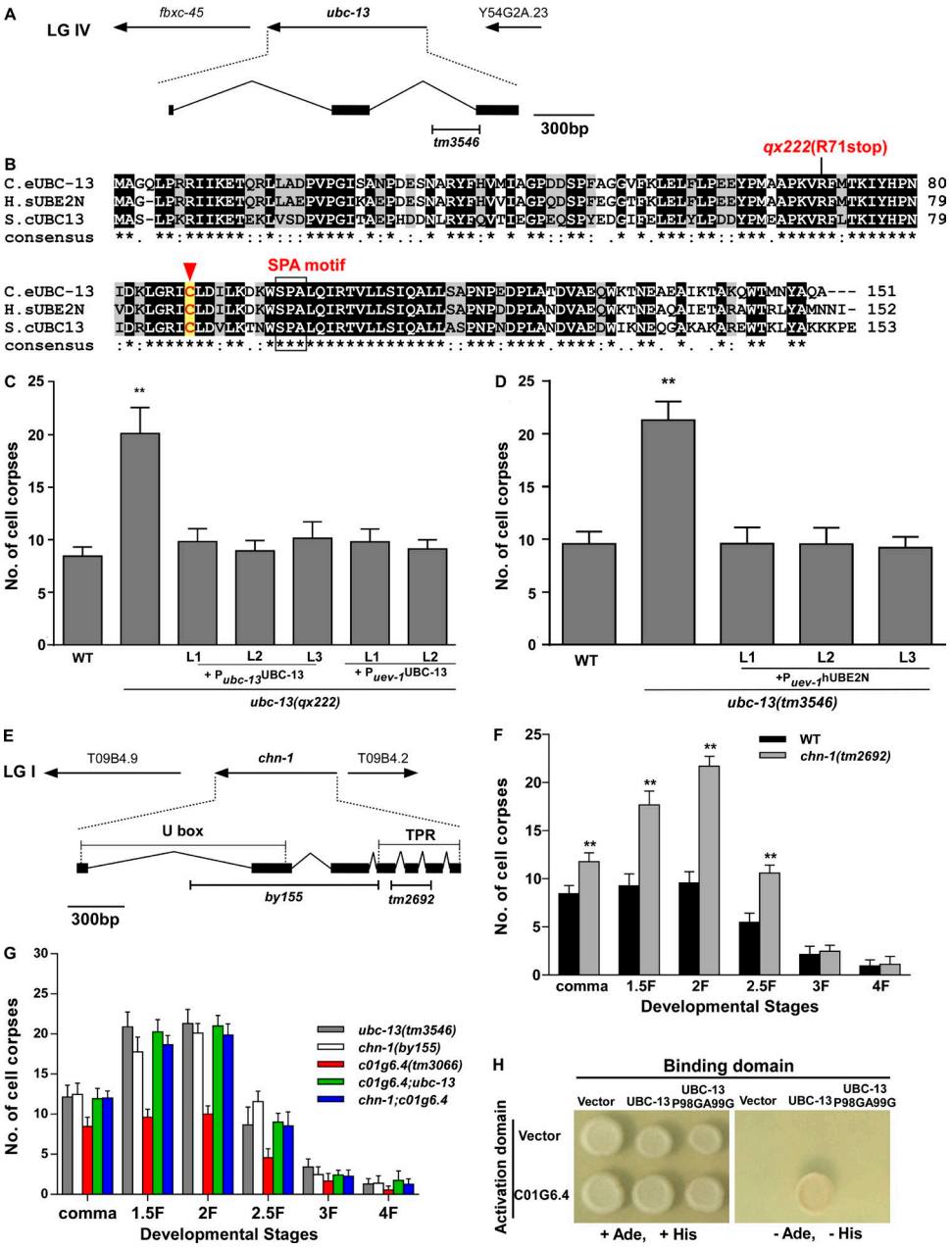

Figure S1. ***qx222*affects the *ubc-13* gene.** (A) The location and gene structure of *ubc-13*. Black boxes show coding segments. The deletion site in the *tm3546* allele is indicated. (B) Sequence alignment of *C. elegans* (C.e) UBC-13, human (H.s) UBE2N, and yeast (S.c) UBC13. Identical residues are shaded in black and similar ones in gray. Red arrowhead indicates the catalytic cysteine residue essential for E2 activity. The SPA motif required for binding with E3 ligases and the mutation identified in the *qx222* allele are also indicated. (C and D) The cell corpse phenotype of *ubc-13(lf)* mutants can be rescued by expressing *ubc-13* or human *UBE2N*. Cell corpses from two or three independent transgenic lines (L1, L2, and/or L3) were scored at the twofold embryonic stage. At least 15 embryos were scored in each strain. Data are shown as mean ± SD. One-way ANOVA with Tukey's posttest was performed to compare mutant datasets (with or without transgene expression) with WT. **, $P < 0.0001$; all other points have $P > 0.05$. (E) The location and gene structure of *chn-1*. Black boxes show coding segments. The domain structure of CHN-1 and deletion sites in *by155* and *tm2692* alleles are indicated. (F and G) Time course analysis of cell corpses during embryonic development was performed in the indicated strains. At least 15 embryos were scored at each stage. Data are shown as mean ± SD. Data derived from different genetic backgrounds at multiple developmental stages were compared by two-way ANOVA followed by Bonferroni posttest. Mutant datasets were compared with WT (F), and datasets from double mutants were compared with single mutants (G). **, $P < 0.001$; all other points have $P > 0.05$. (H) In a yeast two-hybrid assay, the E3 ubiquitin ligase C01G6.4 interacts with UBC-13 but not UBC-13(P98GA99G), which contains mutations in the SPA motif required for binding E3.

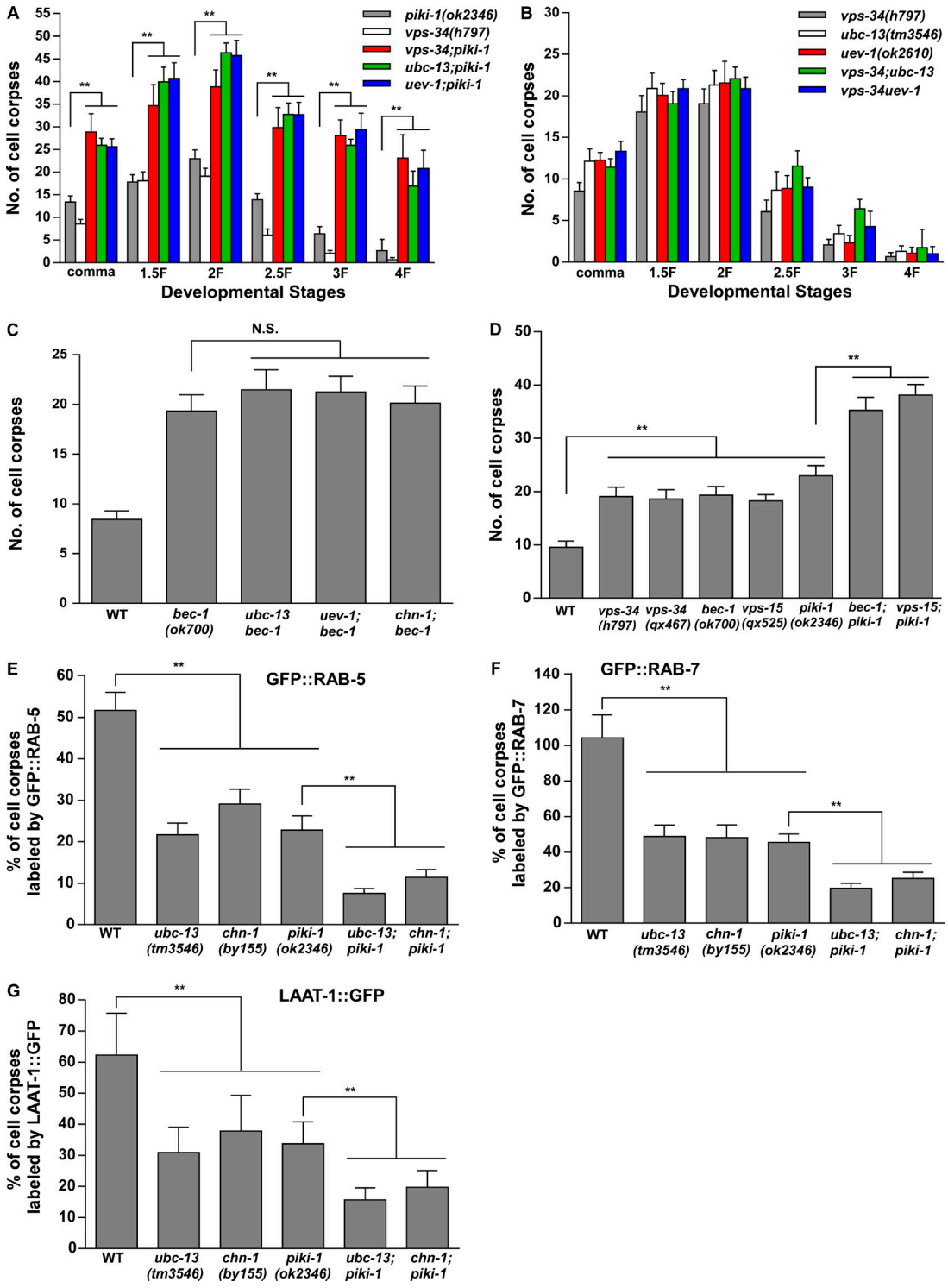

Figure S2. ***ubc-13, uev-1,* and *chn-1* act in the same pathway with *vps-34* but in parallel to *piki-1* to promote cell corpse removal.** (A–D) Cell corpse appearance was analyzed during embryonic development (A and B) or at the twofold embryonic stage (C and D) in the indicated strains. At least 15 embryos were scored at each stage in each strain. Data are shown as mean ± SD. Two-way ANOVA with the Bonferroni posttest (A and B) or one-way ANOVA with Tukey's posttest (C and D) was performed to compare datasets that are linked by lines (A, C, and D) or datasets from double mutants with single mutants (B). **, $P < 0.001$ (A); **, $P < 0.0001$ (D); N.S., no significance. All points in B have $P > 0.05$. (E–G) The percentage of cell corpses labeled by GFP::RAB-5 (E), GFP::RAB-7 (F), or LAAT-1::GFP (G) was quantified in the indicated strains. At least 15 embryos at the twofold stage were scored in each strain. Data are shown as mean ± SD. One-way ANOVA with Tukey's posttest was performed to compare datasets that are linked by lines. **, $P < 0.0001$.

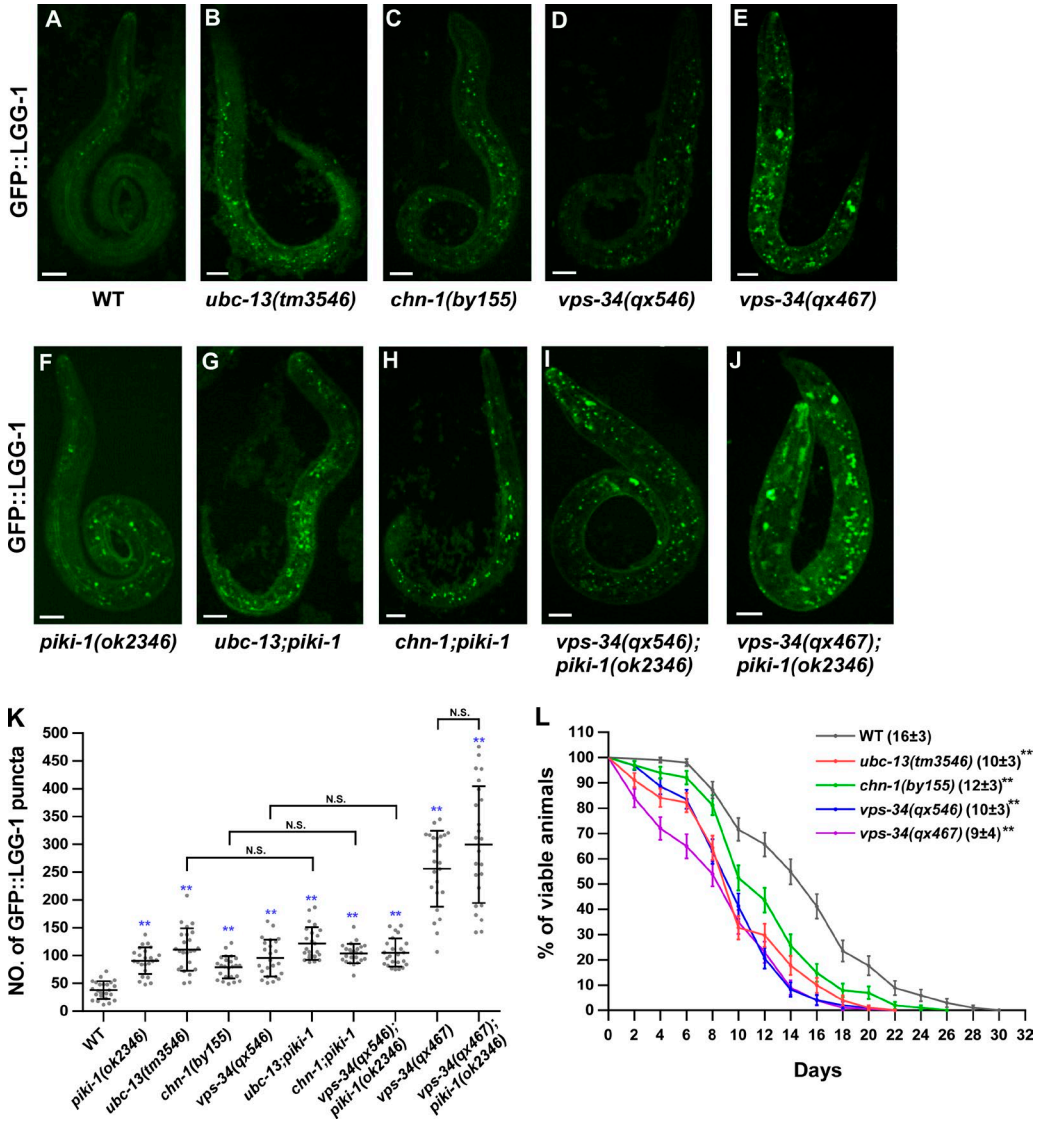

Figure S3. **Loss of *ubc-13* and *chn-1* partially impairs autophagy.** (A–J) Confocal fluorescent images of L1 larvae expressing GFP::LGG-1 in the indicated strains. Bars, 10 µm. Quantification is shown in K. At least 20 animals were scored in each strain. (L) The survival of L1 larvae in the absence of food was quantified in the indicated strains. At least 600 animals were scored each day. In K and L, data are shown as mean ± SD. One-way ANOVA with Tukey's posttest was performed to compare mutant datasets with WT, and the unpaired *t* test was used to compare datasets that are linked by lines in K. In L, the Kaplan-Meier method followed by the log-rank test was performed to compare mutant datasets with WT. **, $P < 0.0001$; N.S., no significance.

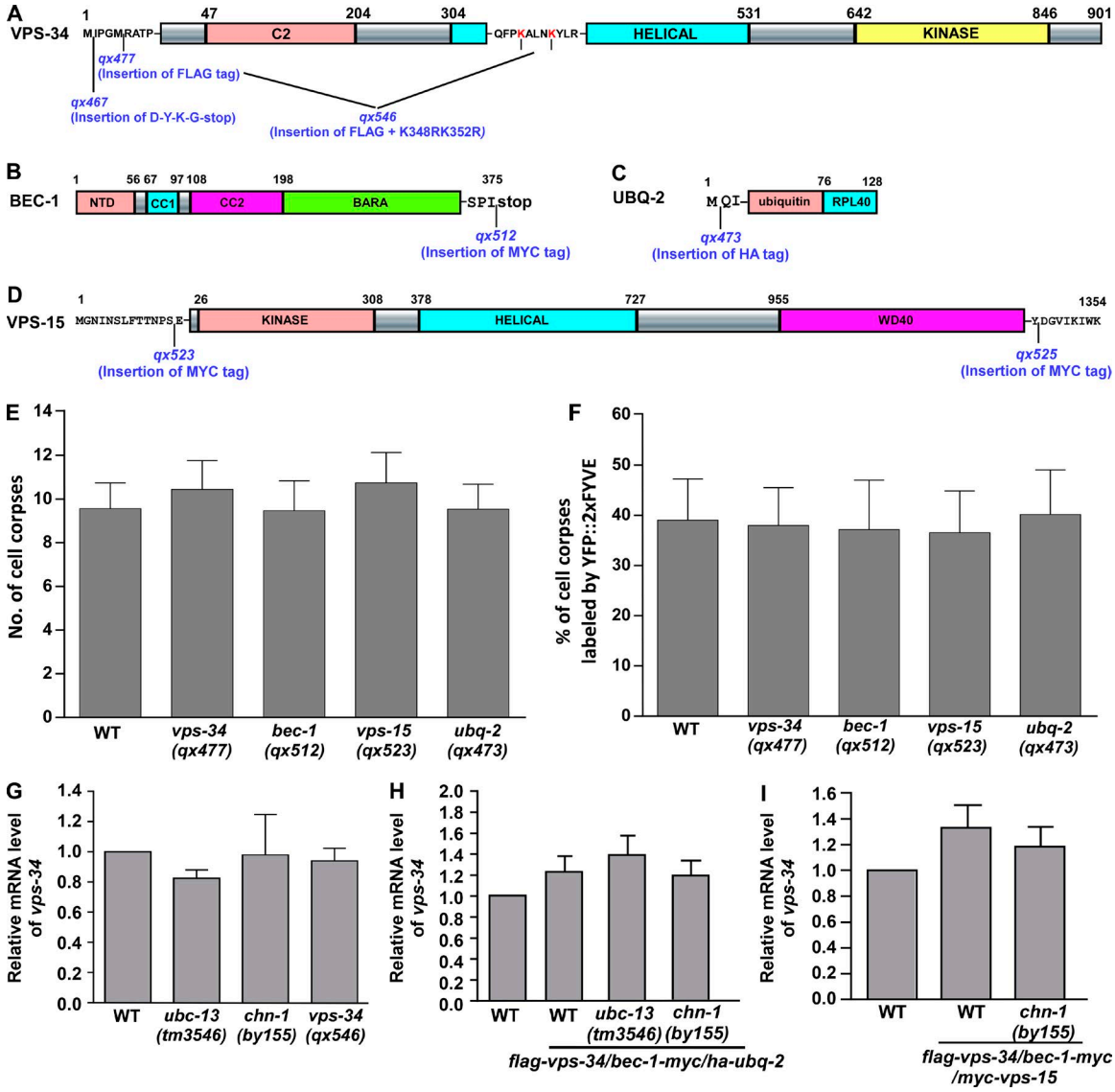

Figure S4. **Use of CRISPR-Cas9 to generate mutation and tag insertion alleles of *vps-34*, *bec-1*, *vps-15*, and *ubq-2*.** (A–D) Schematic illustration of the mutation and tag insertions generated by CRISPR-Cas9 editing of the endogenous *vps-34* (A), *bec-1* (B), *ubq-2* (C), and *vps-15* (D) loci. The amino acids near the insertion or mutation sites are indicated. The *vps-34(qx546)* allele was generated by mutating lysine residues 348 and 352 to arginine in *qx477* worms. (E and F) Cell corpses (E) and YFP::2xFYVE labeling (F) were scored at the twofold embryonic stage in the indicated strains. At least 15 embryos were scored in each strain. Data are shown as mean ± SD. One-way ANOVA with Tukey's posttest was performed to compare tag insertion strains with WT. All points have $P > 0.05$. (G–I) The mRNA level of *vps-34* was quantified by quantitative RT-PCR in the indicated strains. *act-1* was used as the internal reference. At least three independent experiments were performed. Data are shown as mean ± SD and were compared using the unpaired *t* test. All points have $P > 0.05$.

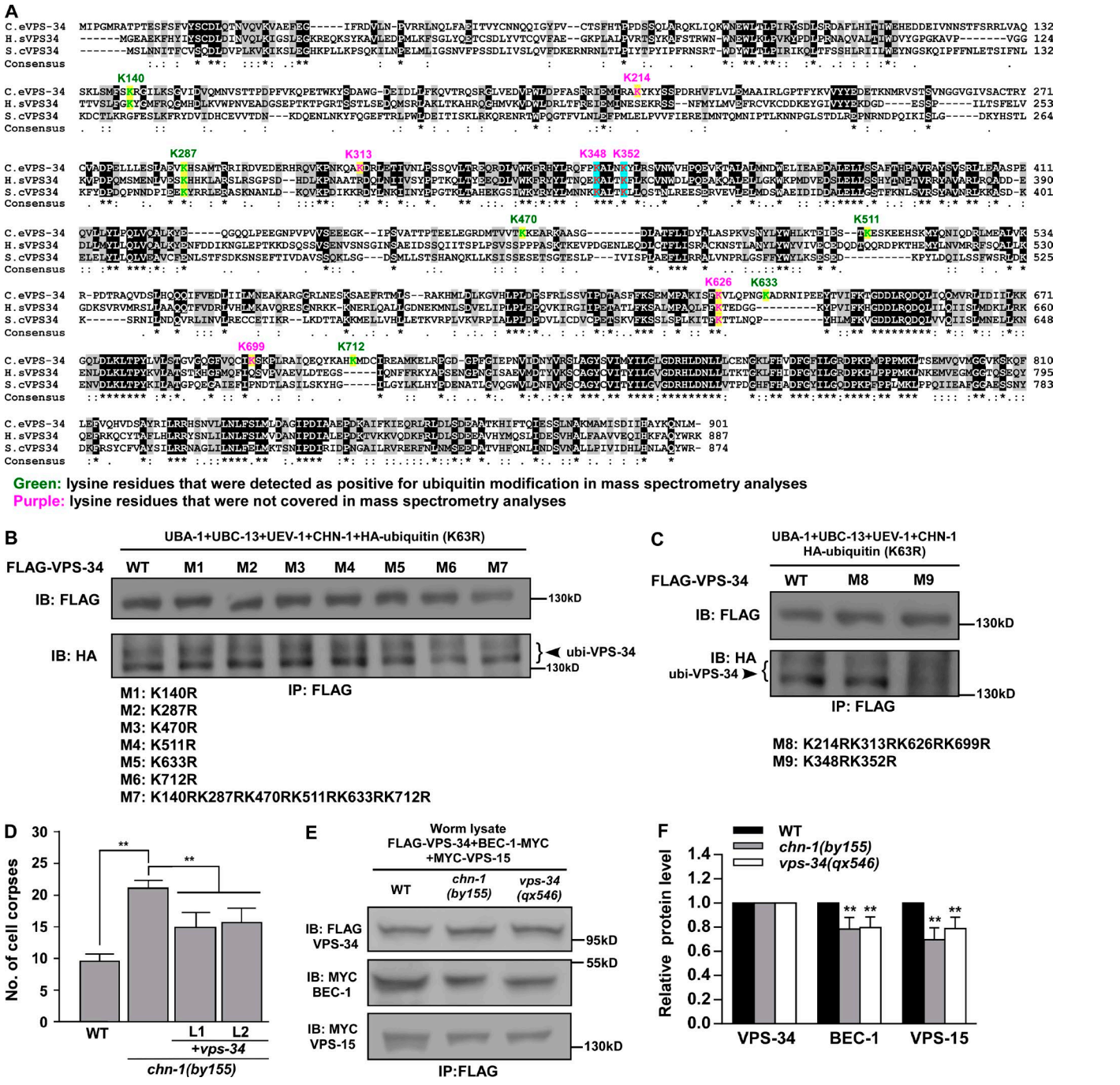

Figure S5. **Lysine residues 348 and 352 are important for the ubiquitination of VPS-34.** (A) Sequence alignment of *C. elegans* (C.e) VPS-34, human (H.s) VSP34, and yeast (S.c) VPS34. Identical residues are shaded in black and similar ones in gray. The lysine residues in green were detected as positive for ubiquitin modification in MS. Lysine residues in purple were not covered in the MS analyses. (B and C) Mono-ubiquitination of WT and various mutated forms of VPS-34 was examined in vitro using K63R-ubiquitin. Mutations in lysine residues 348 and 352 but not in other lysine residues disrupt ubiquitination of VPS-34 in vitro. IB, immunoblot. (D) Overexpression of *vps-34* partially rescued the cell corpse phenotype in *chn-1(by155)* mutants. Cell corpses from two independent transgenic lines (L1 and L2) at the twofold embryonic stage are quantified. At least 15 embryos were scored in each strain. Data are shown as mean ± SD. One-way ANOVA with Tukey's posttest was performed to compare datasets that are linked by lines. **, $P < 0.0001$. (E and F) VPS-34 association with BEC-1 and VPS-15 is reduced in *chn-1(by155)* and *vps-34(qx546)* mutants. Lysates were prepared from WT, *chn-1(by155)*, and *vps-34(qx546)* worms carrying *flag::vps-34, bec-1::myc*, and *myc::vps-15* alleles. FLAG IP was performed followed by detection of VPS-34, BEC-1, and VPS-15 by anti-FLAG and anti-MYC antibodies. The graphs in F show the relative protein levels, quantified using ClinX Image Analysis as mean ± SD of three independent sets of experiments. FLAG–VPS-34 was the loading control. Mutant datasets were compared with WT using the unpaired *t* test. **, $P < 0.0001$.

Table S1. **Strains that were used in this work**

Gene/locus	Allele	Genomic changes	Protein changes	Linkage group
uev-1	*ok2610*	Deletion	Deletion	LG I
vps-34	*h797*	Substitution	Missense	LG I
	qx467	Insertion	Premature stop	LG I
	qx546	Insertion/Substitution	FLAG insertion/K348RK352R	LG I
chn-1	*by155*	Deletion	Deletion/premature stop	LG I
	tm2692	Deletion/Insertion	Deletion	LG I
c01g6.4	*tm3066*	Deletion	Deletion/premature stop	LG II
vps-15	*qx523*	Insertion	MYC tag insertion	LG II
	qx525	Insertion	MYC tag insertion	LG II
ubq-2	*qx473*	Insertion	HA tag insertion	LG III
ubc-13	*qx222*	Substitution	Premature stop	LG IV
	tm3546	Deletion	Deletion/premature stop	LG IV
bec-1	*ok700*	Deletion/Insertion	Deletion	LG IV
	qx512	Insertion	MYC tag insertion	LG IV
cxTi10882	*qxSi13*	Insertion	$P_{lgg\text{-}1}$GFP::LGG-1	LG IV
piki-1	*ok2346*	Deletion	Deletion	LG X
gfp::rab-5	*qxIs408*	Integration	GFP::RAB-5	ND
gfp::rab-7	*qxIs66*	Integration	GFP::RAB-7	ND
laat-1::gfp	*qxIs354*	Integration	LAAT-1::GFP	ND
ced-1::gfp	*smIs34*	Integration	CED-1::GFP	ND
yfp::2xfyve	*opIs334*	Integration	YFP::2xFYVE	ND

LG, linkage group; ND, not determined.